

**THE OPERATIONAL HIGH RESOLUTION WINDOW WRF MODEL  
RUNS AT NCEP: ADVANTAGES OF MULTIPLE MODEL RUNS  
FOR SEVERE CONVECTIVE WEATHER FORECASTING**

Steven J. Weiss<sup>1</sup>, Matthew E. Pyle<sup>2</sup>, Zavis Janjic<sup>2</sup>, David R. Bright<sup>1</sup>,  
John S. Kain<sup>3</sup>, and Geoffrey J. DiMego<sup>2</sup>

<sup>1</sup> NOAA/NWS/NCEP Storm Prediction Center, Norman, Oklahoma

<sup>2</sup> NOAA/NWS/NCEP Environmental Modeling Center, Camp Springs, Maryland

<sup>3</sup> NOAA/OAR National Severe Storms Laboratory, Norman, Oklahoma

## 1. INTRODUCTION

In April 2004, the National Centers for Environmental Prediction (NCEP) Environmental Modeling Center (EMC) began running a once daily experimental high resolution version of the Weather Research and Forecasting (WRF) model with the Non-hydrostatic Mesoscale Model (NMM) dynamic core (Janjic 2003; Janjic et al. 2005). The WRF-NMM was integrated out to 36 hr over a large domain (three-fourths Continental United States, or CONUS) with 4.5 km grid length and with no parameterized convection for testing and evaluation in the NOAA Hazardous Weather Testbed (HWT) 2004 Spring Experiment. The Spring Experiment is highly collaborative activity organized annually by the Storm Prediction Center (SPC) and National Severe Storms Laboratory to bring together numerical model developers, research scientists, operational forecasters, and university faculty and students to accelerate the transfer of cutting edge research to National Weather Service operations. A primary goal of the HWT interactions is to improve forecasts and warnings of hazardous weather such as severe convective storms and flood producing rainfall. For more information about the HWT Spring Experiments, see Kain et al. (2003a; 2003b).

Feedback about the performance of the WRF-NMM during the 2004 Spring Experiment was very positive, indicating that convection-allowing WRF models had the capability to provide unique guidance to forecasters on important details of thunderstorm characteristics such as convective initiation, evolution, and convective mode, even at forecast times as long as 36 hr (Kain et al. 2006). In particular, aspects of convective mode are very important to severe weather forecasters, as the type of severe weather that occurs (e.g., tornadoes, large hail, or damaging thunderstorm winds) is often related to the mesoscale or storm scale configuration of the convection (Trapp et al. 2005; Gallus et al. 2008; Thompson et al. 2008; Smith et al. 2008). For example, tornadoes are more frequently associated with discrete supercells, whereas convective wind damage is more common with quasi-linear systems, including bow echoes. As a result of the initial evaluation findings, EMC continued running an experimental version of the model year round to provide support for SPC

forecasters. Periodic improvements to the WRF-NMM have been made since then, including a decrease in grid length to 4 km, upgrades to newer WRF versions, modifications to model physics, and the creation of additional specialized convective products.

One key challenge in severe thunderstorm forecasting is predicting the evolution of nocturnal convection that occurs prior to the onset of the next day's diurnal heating cycle. This routinely impacts operational forecasters issuing next day severe weather forecast products, especially from the Plains states into the Mississippi Valley during the warm season when the frequency of overnight thunderstorms is maximized (e.g., Easterling and Robinson 1985; Carbone and Tuttle 2008). The progression and degree of persistence of nocturnal storms can result in modification of the convective environment well into the next afternoon, influencing a variety of factors such as the location of low-level boundaries, amount of cloud cover and resultant solar insolation, and air mass thermodynamic characteristics in the wake of the convectively generated cold pool. Thus, a skillful severe weather forecast for the upcoming day is often dependent on properly predicting the evolution of overnight storms and determining of their effects, if any, during the upcoming diurnal cycle.

It has been found that the ability of WRF-model forecasts initialized at 00 UTC to provide useful guidance to severe weather forecasters is partially dependent on how well the model predicts the evolution of overnight storms early in the model integration (Kain et al. 2008a; Coniglio 2008). For example, erroneous persistence of model generated deep convection that persists beyond the time observed convection dissipates often results in excessive stabilization of the local boundary layer and development of convective outflow boundaries that are not present in the actual atmosphere. When this happens, subsequent model development of thunderstorms may occur along the spurious boundary and destabilization may be inhibited within the model generated cold pool. In this situation, the model's poor representation of the mesoscale environment makes accurate prediction of subsequent convective activity less likely.

In the fall of 2007, a version of the 4 km WRF-NMM was implemented in the NCEP High Resolution Window (HiResW) operational run slot, along with a version of the Advanced Research WRF (WRF-ARW; Skamarock

---

\* Corresponding author address: Steven J. Weiss, NOAA Storm Prediction Center, 120 David L. Boren Blvd., Norman, OK 73072; e-mail: steven.j.weiss@noaa.gov

et al. 2005) run with a 5.1 km grid length. Over the CONUS, these two WRF configurations are run twice daily (at 00 and 12 UTC) over an eastern two-thirds CONUS domain, and once daily at 06 UTC over a western two-thirds CONUS domain, with all runs producing forecasts out to 48 hr. The geographic areas covered by the HiResW WRF runs for the CONUS are shown in Fig. 1. The introduction of 12 UTC WRF runs in the HiResW should, in principle, provide forecasters with improved guidance for afternoon and evening thunderstorm development, since they are initialized with later observational data at the start of a new diurnal cycle.

This study examines several cases of significant severe weather occurrence during the spring and early summer of 2008, and compares the guidance from the 00 UTC and 12 UTC HiResW WRF-NMM runs. The 00 UTC WRF-NMM model output has been used routinely by SPC forecasters for a number of years and they are familiar with its performance characteristics, so it is important to see if the 12 UTC update run provides improved guidance owing to its later initialization time.

## 2. HiResW WRF-NMM MODEL

The WRF-NMM is nested within the 12 km North American Mesoscale (NAM) model. It is configured with 35 vertical levels and the following physical parameterizations: MYJ turbulence/PBL, Ferrier microphysics, and GFDL shortwave and longwave radiation. The model is “cold started” using NAM initial and lateral boundary conditions that are interpolated to the WRF-NMM 4 km grid. Because of the cold start, there is typically a spin-up period of approximately 4-6 hours before the WRF-NMM develops stable, coherent precipitation systems, such that the forecast guidance is most useful for time periods beyond 6-12 hours. Previous experiences with 00 UTC convection-allowing WRF models have focused on forecasts for the next afternoon and evening, or 18-30 hours into the model integration, where subjective (e.g., Done et al. 2004; Weisman et al. 2008; Weiss et al. 2007; Kain et al. 2008b) and objective (Schwartz et al. 2008) evaluations have shown that the models can, at times, provide very useful guidance for afternoon and evening thunderstorm activity. A similar spin-up period is evident in the 12 UTC WRF-NMM, so it should not be expected to provide useful guidance on thunderstorms until the afternoon time period (18-00 UTC) at the earliest, which coincides with the peak in the diurnal heating cycle.

Specialized convective output fields from convection-allowing models such as simulated reflectivity have been developed to better depict model generated storms (Koch et al. 2005). Forecasters have found the simulated reflectivity fields to be very useful, in large part because the model output then provides views of storms that are very similar to convective storms as seen on radar displays. The use of simulated reflectivity allows forecasters to see mesoscale and near storm scale details of model generated convection

(i.e., bow echo and supercell structures) that can indicate potentially severe storms. It also facilitates visual comparison of model forecasts with observed radar for subjective verification purposes. The latter approach will be employed during the examination of several severe weather cases in the next section.

## 3. CASE EXAMPLES

Several examples are presented that illustrate potential advantages of multiple WRF-NMM runs at 12 hour intervals. These cases consist of active severe weather episodes that occurred across different parts of the central and eastern United States during May and June of 2008, during which determination of the convective details was an important aspect of the forecasting challenge.

### 3.1 2 May 2008: Mid South/Lower Mississippi Valley

Widespread severe thunderstorms spread across the Mid-South and lower Mississippi Valley through much of the day and into the night (Fig. 2), with killer tornadoes striking parts of Arkansas during the morning resulting in six fatalities. The severe storms were initially part of a quasi-linear convective system that moved across parts of Missouri, northwest Arkansas, and Oklahoma during the overnight hours, then continued into the lower Mississippi valley during the afternoon and evening.

The 13 UTC 2 May radar mosaic of base reflectivity showed a quasi-linear convective system with several larger scale bowing structures extending from east central Missouri into northern Arkansas and northeast Texas (Fig. 3). The 00 UTC WRF-NMM 13 hr forecast valid at that time (Fig. 4) predicted a linear system similar to the observational data, although the model was too slow with the eastward progression of the line across Missouri and northern Arkansas. The model forecast also included spurious strong storms across northern Louisiana, and more extensive convection compared to observations from northeast Arkansas into southeast Missouri. These latter storms may have corresponded to the isolated thunderstorms observed over southwest Tennessee and far western Kentucky. The model forecast continued to over-predict the erroneous downstream storms eastward across the Mississippi river through the remainder of the morning, and these storms generated an expanding low level cold pool that stabilized the model environment ahead of the advancing line of storms moving across Arkansas (Fig. 5). The line subsequently weakened in the model forecast, and the focus for new intense storms was along the spurious outflow boundary from northern Louisiana into central Mississippi by 00 UTC 3 May (Fig. 6). The actual storms continued eastward to produce substantial severe weather across eastern Arkansas, western Tennessee, and northern Mississippi into the early evening (Fig. 7).

The 12 UTC WRF-NMM required several hours of integration time to spin-up convective storms, but during this time it did not generate significant storms across northern Louisiana and eastern Arkansas (Fig. 8). As a result, the model atmosphere destabilized considerably over eastern Arkansas and west Tennessee ahead of the model storms (Fig. 9), and the 12 UTC WRF-NMM simulated reflectivity forecasts indicated the Arkansas storms would remain intense as they progressed eastward through the afternoon (Fig. 10). It appears that the improved convective storm guidance from the 12 UTC WRF-NMM resulted from a more realistic forecast of instability compared to the run from 12 hours earlier, and this more favorable thermodynamic environment supported the development of model storms that more closely resembled the evolution of the actual storms.

### **3.2 June 2008: Middle Atlantic States and Central Plains**

Very significant severe weather occurred over two regions of the CONUS on 4 June 2008, and each area will be examined separately.

#### **3.2.1 Middle Atlantic States**

Several episodes of severe thunderstorms moved rapidly eastward from southern Ohio across West Virginia and the Delmarva region, causing widespread significant wind damage and tornadoes across northern Virginia, the District of Columbia (DC), and northern Maryland (Fig. 11). The initial bow echo system moved into the DC area around 19 UTC (Fig. 12), while the second severe weather producing system developed along and immediately north of an outflow boundary established by the first system. The second convective system became better organized as it moved through the DC area around 00 UTC 5 June (Fig. 13). The WRF-NMM initialized at 00 UTC 4 June provided very useful guidance showing gradually intensifying storms as they moved from Ohio into northern Virginia, culminating in a bowing convective system moving rapidly across the region,. Although the model forecast was approximately two hours slow moving the bow echo system across the DC region (Fig. 14), the overall track and mesoscale configuration of the initial convective system was well predicted. However, the convectively generated cold pool and outflow boundary produced by the first system spread too far south into southern Virginia (Fig. 15), and subsequent model storms that developed in the marginally unstable environment north of the boundary were too weak (Fig. 16) compared with observed radar (Fig. 13).

Unlike the 00 UTC WRF-NMM, the 12 UTC model run did not predict the initial bow echo convective system during the afternoon (Fig. 17), as the model developed storms too far north across Pennsylvania. However, the morning update run did produce a bow echo system moving across northern Virginia and the DC area around 00-01 UTC during the time the second

severe weather system affected the region (Fig. 18). For this run, the spin-up time during the first 4-6 hours of the integration coincided with the initial storms moving rapidly across the region, and it appears that the model was unable to “catch up” to reality in the early part of the forecast period.

It is also instructive to examine the relationship between the NAM model, which provides the initial and lateral boundary conditions for the WRF-NMM, and the WRF-NMM forecasts themselves. Weisman et al. (2008) and Kain et al. (2008a) have noted a correspondence between the forecasts from the NAM and convection-allowing models, suggesting that the forcing for large scale and mesoscale ascent provided by the NAM can have a strong influence on the development of convective storms in the high resolution model. Figs. 19-20 show the 3-hr accumulated precipitation valid at 21 UTC 3 May from the 00 UTC and 12 UTC NAM forecasts, respectively. The placement of precipitation in the NAM forecasts is similar to the location of convective storms in the WRF-NMM forecasts (compare Figs. 14 and 19, and Figs. 17 and 20), and the general correspondence between the larger scale NAM and the WRF-NMM forecasts continued through the evening hours (not shown). These findings clearly suggest that the larger scale background forcing provided by the NAM likely played a role in the WRF-NMM forecasts of convective storms. The influence of the larger scale background fields help to explain why convection-allowing models tend to produce more useful forecasts of near-storm scale details in strongly forced situations, which is when mesoscale models typically exhibit greater skill. Conversely, if there are errors in placement and intensity of forcing in the larger scale model, as illustrated by the precipitation forecast from the 12 UTC 4 June NAM model, the errors may be reflected by the higher resolution model as well.

In this case, neither the 00 UTC nor the 12 UTC WRF-NMM run were able to capture accurately the entire sequence of multiple convective systems, but each was able to predict reasonably well one convective system that corresponded to the observations. This complex episode illustrates some of the challenges forecasters have in interpreting and utilizing convection-allowing model guidance for operational severe weather forecasting. For example, real-time comparisons between observations and forecasts of thunderstorms from the 00 UTC WRF-NMM during the morning of 4 June showed that the model was largely replicating reality on the mesoscale. That information would have provided a forecaster with confidence that a significant convective system was likely to move across the Delmarva region, but with more limited storms in its wake. Conversely, given the poor model performance of the 12 UTC run by early afternoon, most forecasters would have discounted the convective storm guidance it provided. However, the update run did eventually develop a bowing convective system across the region

that corresponded well in time and space with the second convective system.

### **3.2.2 Central Plains**

Severe thunderstorms developed initially during the afternoon of 4 June 2008 over northeast Colorado, and other severe storms developed explosively during the mid-late afternoon near an east-west warm front across southern Nebraska and southwest Iowa (Fig. 21). Numerous reports of tornadoes, very large hail, and significant wind gusts were concentrated along a narrow corridor from northeast Colorado across Nebraska into southwest Iowa (see Fig. 11). This episode exemplifies the challenges associated with nocturnal convection, as the 00 UTC WRF-NMM maintained a spurious nocturnal bow echo system across eastern Nebraska during the morning hours (Fig. 22), while radar observations showed there had been no storms across this area (not shown). The model storms generated a pronounced cold pool and surface-based stable layer behind an outflow boundary that spread southward well into Kansas (Fig. 23). This largely stable model environment over the central plains persisted through the afternoon hours and strongly inhibited the development of strong convective storms over Nebraska (Fig. 24).

The 12 UTC WRF-NMM did not develop storms over central or eastern Nebraska into the early afternoon (Fig. 25) and the model environment underwent strong destabilization during this time period (Fig. 26). This is similar to what had occurred in the actual atmosphere. Although the 12 UTC run developed storms over Nebraska 1-2 hours late compared to radar, it still provided very useful guidance to forecasters on the widespread intense storms that developed across Nebraska (Fig. 27). For this severe weather episode, the 12 UTC update run was able to correct for the erroneous nocturnal convection generated by the 00 UTC WRF-NMM, and as a result, it provided much improved guidance for a region where significant convection did not begin until later in the day.

The 4 June case also points out that model performance is not necessarily uniform across a large model domain, as the 00 UTC WRF-NMM exhibited better (worse) thunderstorm guidance over the Mid-Atlantic states (central plains), whereas the 12 UTC update run performance was reversed for the two geographic regions.

### **3.3 11 June 2008: Central Plains**

Significant severe weather, including numerous reports of tornadoes, developed during the afternoon and evening near a cold front that was moving across parts of western Iowa, eastern Nebraska, and Kansas (Fig. 28). Killer tornadoes struck a Boy Scout camp in western Iowa during the early evening, and additional killer tornadoes went through two small towns in Kansas later in the evening.

WRF-NMM convective forecasts from the 00 UTC and 12 UTC runs on 11 June provided consistent guidance, with both models moving morning convection northeastward across Iowa and the upper Mississippi valley, and predicting substantial destabilization in the wake of the morning storms prior to the arrival of the cold front (not shown). Both model runs also developed similar quasi-linear or band of convective systems near the cold front during the late afternoon and evening hours (Figs. 29-30), although a narrower linear structure was evident in the 00 UTC run. Overall, the mesoscale evolution of the model storms corresponded well with radar observations (Fig. 31), as the models developed intense storms in nearly identical locations and times. The larger scale models including the NAM had exhibited considerable run-to-run consistency in the synoptic and mesoscale pattern and environment for several days leading up to this event. NAM forecasts from 00 and 12 UTC 11 June continued this trend by focusing heavier precipitation along the cold front during the evening (Figs. 32-33).

The run-to-run consistency of the larger scale NAM forecasts coupled with similarities in the convective forecasts from the WRF-NMM runs suggest that the larger scales may have been more predictable in this case. The enhanced synoptic and mesoscale predictability was reflected by the similar thunderstorm configurations produced by the 00 and 12 UTC WRF-NMM forecasts. In these types of situations, forecaster confidence in the WRF-NMM solutions is likely to be increased given the consistent solutions offered by the models.

## **4. SUMMARY AND DISCUSSION**

The updated 12 UTC WRF-NMM model runs in the HiResW have been found to provide improved thunderstorm guidance to severe weather forecasters for the afternoon and evening time period on some occasions during the spring and early summer of 2008. When the 00 UTC WRF-NMM erroneously predicted the persistence of nocturnal convection into the next diurnal heating cycle, local recovery of the model's boundary layer was suppressed and convectively induced outflow boundaries were often misplaced. As a result, subsequent convective development was sometimes focused in the wrong area or suppressed altogether. In these situations, updated initial conditions in the 12 UTC WRF-NMM were more likely to properly reflect the convective environment, and forecasts from the update run often provided improved guidance for severe weather forecasters. Conversely, when overnight convection diminished or dissipated before 12 UTC and/or the 00 UTC run predicted reasonably well the overnight convection and associated modifications of the environment, the forecast guidance from the 00 UTC run was more likely to have utility to forecasters. Finally, when the thunderstorm guidance from the 12 UTC run was similar to that from the previous 00 UTC run, forecasters were able to have more confidence in the model solutions.

It was also seen that the influence of the larger scale forcing for ascent provided by the NAM model can be rather pronounced in some instances. Thus, forecasters are advised to compare forecasts from the NAM and the nested WRF-NMM on a routine basis, as this comparison may provide useful insights into why the WRF-NMM is focusing convective storms in specific areas.

These results highlight the importance of incorporating improved initial conditions at the start of the diurnal heating cycle into updated convection-allowing WRF models, especially during periods of active overnight thunderstorms. They also suggest that high resolution models capable of providing guidance for smaller scale, high impact weather events may need to be run on an increasingly frequent basis to take advantage of later observational data that will be incorporated into the initial conditions of the updated model runs.

## ACKNOWLEDGMENTS

We thank Gregory Grosshans (SPC) for his assistance in establishing the High Resolution Window model data flow into the SPC, and Eric Rogers and Tom Black (both at EMC) for their long-term development work on the WRF-NMM model. The expertise of Linda Crank (SPC) to finalize the format of the paper is greatly appreciated.

## 5. REFERENCES

- Coniglio, M. C., J. S. Kain, S. J. Weiss, D. R. Bright, J. J. Levit, G. W. Carbin, K. W. Thomas, F. Kong, M. Xue, M. L. Weisman, and M. E. Pyle, 2008: Evaluation of WRF model output for severe-weather forecasting from the 2008 NOAA Hazardous Weather Testbed Spring Experiment. *Preprints, 24th Conference on Severe Local Storms*, Amer. Meteor. Soc., Savannah, GA. CD-ROM 12.4.
- Carbone, R. E. and J. D. Tuttle, 2008: Rainfall occurrence in the U.S. warm season: The diurnal cycle. *J. Climate*, **21**, 4132–4146.
- Done J., C. A. Davis, and M. L. Weisman, 2004: The next generation of NWP: Explicit forecasts of convection using the Weather Research and Forecasting (WRF) model. *Atmos. Sci. Lett.*, **5**, 110–117, doi:10.1002/asl.72.
- Easterling, D. R. and P. J. Robinson, 1985: The diurnal variation of thunderstorm activity in the United States. *J. Appl. Meteor.*, **24**, 1048–1058.
- Gallus, W. A. Jr., N. A. Snook, and E. V. Johnson, 2008: Spring and summer severe weather reports over the Midwest as a function of convective mode: A preliminary study. *Wea. Forecasting*, **23**, 101–113.
- Janjic, Z. I., 2003: A nonhydrostatic model based on a new approach. *Meteorology and Atmospheric Physics*, **82**, 271–285.
- Janjic, Z., T. Black, M. Pyle, E. Rogers, H.-Y. Chuang, and G. DiMego, 2005: High resolution applications of the WRF NMM. *Preprints, 21st Conference on Weather Analysis and Forecasting/17th Conference on Numerical Weather Prediction*, Amer. Meteor. Soc., Washington, DC. CD-ROM 16A.4.
- Kain, J. S., P. R. Janish, S. J. Weiss, M.E. Baldwin, R. S. Schneider, and H. E. Brooks, 2003a: Collaboration between forecasters and research Scientists at the NSSL and SPC: The spring program. *Bull. Amer. Meteor. Soc.*, **84**, 1797–1806
- Kain, J. S., M. E. Baldwin, P. R. Janish, S. J. Weiss, M. P. Kay, and G. W. Carbin, 2003b: Subjective verification of numerical models as a component of a broader interaction between research and operations. *Wea. Forecasting*, **18**, 847–860.
- Kain, J. S., S. J. Weiss, J. J. Levit, M. E. Baldwin, and D. R. Bright, 2006: Examination of convection-allowing configurations of the WRF model for the prediction of severe convective weather: The SPC/NSSL spring program 2004. *Wea. Forecasting*, **21**, 167–181.
- Kain, J. S., S. J. Weiss, S. R. Dembek, J. J. Levit, D. R. Bright, J. L. Case, M. C. Coniglio, A. R. Dean, R. A. Sobash, and C. S. Schwartz, 2008a: Severe-weather forecast guidance from the first generation of large domain convection-allowing models: Challenges and opportunities. *Preprints, 24th Conference on Severe Local Storms*, Amer. Meteor. Soc., Savannah, GA. CD-ROM 12.1
- Kain, J. S., S. J. Weiss, D. R. Bright, M. E. Baldwin, J. J. Levit, G. W. Carbin, C. S. Schwartz, M. L. Weisman, K. K. Droegemeier, D. B. Weber, and K. W. Thomas, 2008b: Some practical considerations regarding horizontal resolution in the first generation of operational convection-allowing NWP. *Wea. Forecasting*, **23**, 931–952.
- Koch, S. E., B. Ferrier, M. Stolinga, E. Szoke, S. J. Weiss, and J. S. Kain, 2005: The use of simulated radar reflectivity fields in the diagnosis of mesoscale phenomena from high-resolution WRF model forecasts. *Preprints, 11th Conference on Mesoscale Processes*, Amer. Meteor. Soc., Albuquerque, NM, , CD-ROM, J4J.7
- Skamarock, W.C., J. B. Klemp, J. Dudhia, D. O. Gill, D. M. Barker, W. Wang, J. G. Powers, 2005: A Description of the Advanced Research WRF Version 2. NCAR Tech Note, NCAR/TN-468+STR, 88 pp. [Available from UCAR Communications, P. O. Box 3000, Boulder, CO 80307].

Smith, B. T., J. L. Guyer, and A. R. Dean, 2008: The climatology, convective mode, and mesoscale environment of cool season severe thunderstorms in the Ohio and Tennessee valleys, 1995-2006. *Preprints, 24th Conference on Severe Local Storms*, Amer. Meteor. Soc., Savannah, GA. CD-ROM 13B.7

Thompson, R. L., J. S. Grams, and J. Prentice, 2008: Synoptic environments and convective modes associated with significant tornadoes in the contiguous United States. *Preprints, 24th Conference on Severe Local Storms*, Amer. Meteor. Soc., Savannah, GA. CD-ROM 16A.3

Trapp, R. J., S. A. Tessendorf, E. S. Godfrey, and H. E. Brooks, 2005: Tornadoes from squall lines and bow echoes: Part I: Climatological distribution. *Wea. Forecasting*, **20**, 23-33.

Weisman, M. L., C. Davis, W. Wang, K. W. Manning, and J. B. Klemp, 2008: Experiences with 0-36 h Explicit convective forecasts with the WRF-ARW model. *Wea. Forecasting*, **23**, 407-437.

Weiss, S. J., J. S. Kain, D. R. Bright, J. J. Levit, G. W. Carbin, M. E. Pyle, Z. I. Janjic, B. S. Ferrier, J. Du, M. L. Weisman, and M. Xue, 2007: The NOAA Hazardous Weather Testbed: Collaborative testing of ensemble and convection-allowing WRF models and subsequent transfer to operations at the Storm Prediction Center. *Preprints, 22nd Conference on Weather Analysis and Forecasting/18th Conference on Numerical Weather Prediction*, Amer. Meteor. Soc., Park City, UT. CD-ROM 6B.4

## 6. FIGURES



**Figure 1.** NCEP High Resolution Window model domains showing east CONUS (red) and west CONUS (blue) domains. The Alaska domain is also shown in red.

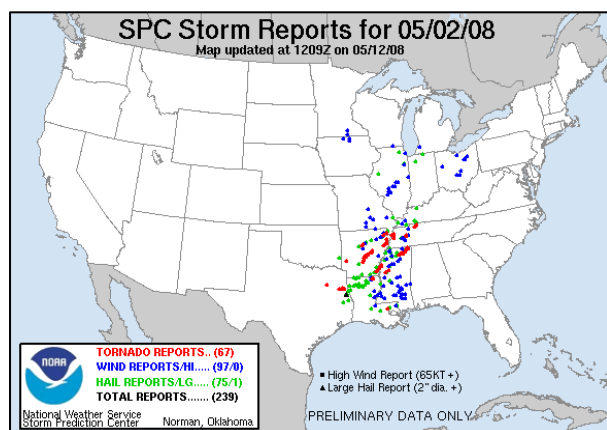


**Figure 2.** Severe weather reports of tornadoes (red), large hail (green), and convective wind damage (blue) from 12 UTC 2 May 2008 to 12 UTC 3 May 2008.



**Figure 3.** Regional radar reflectivity mosaic image at 13 UTC 2 May 2008.



**Figure 4.** 00 UTC 2 May 2008 WRF-NMM 13-hour forecast of simulated reflectivity at 1 km AGL valid 13 UTC 2 May.



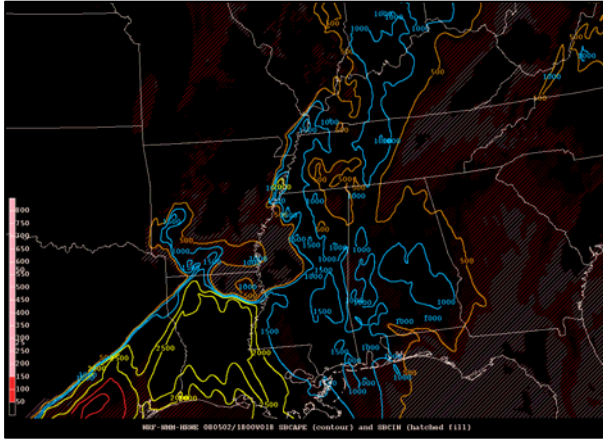


**Figure 5.** 00 UTC 2 May 2008 WRF-NMM 18-hour forecast of surface-based CAPE (contours at  $500 \text{ J kg}^{-1}$  intervals) and CIN (hatched color fill) valid 18 UTC 2 May.



**Figure 8.** 12 UTC 2 May 2008 WRF-NMM 6-hour forecast of simulated reflectivity at 1 km AGL valid 18 UTC 2 May.

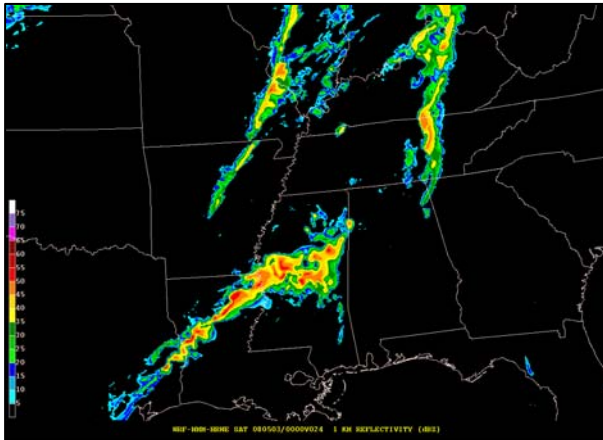


**Figure 6.** 00 UTC 2 May 2008 WRF-NMM 24-hour forecast of simulated reflectivity at 1 km AGL valid 00 UTC 3 May.

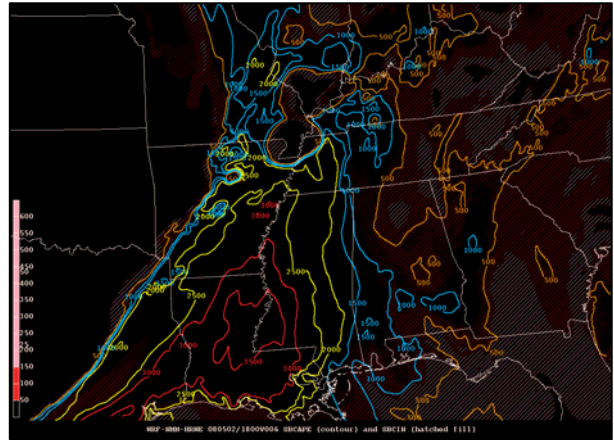


**Figure 9.** 12 UTC 2 May 2008 WRF-NMM 6-hour forecast of surface-based CAPE (contours at  $500 \text{ J kg}^{-1}$  intervals) and CIN (hatched color fill) valid 18 UTC 2 May.

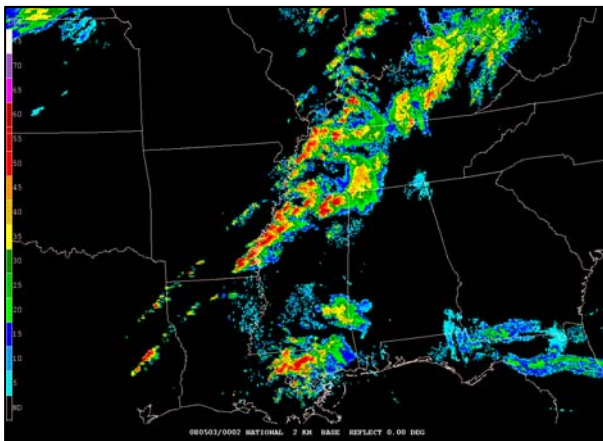


**Figure 7.** Regional radar reflectivity mosaic image at 00 UTC 3 May 2008.

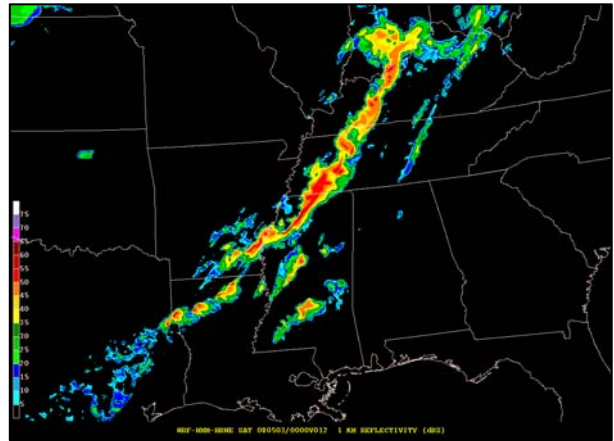


**Figure 10.** 12 UTC 2 May 2008 WRF-NMM 12-hour forecast of simulated reflectivity at 1 km AGL valid 00 UTC 3 May.

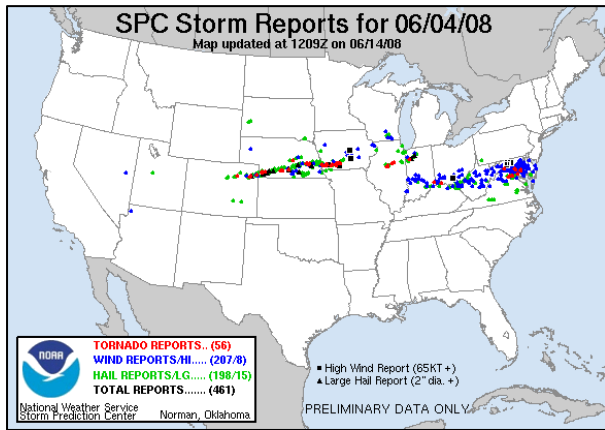


**Figure 11.** Severe weather reports of tornadoes (red), large hail (green), and convective wind damage (blue) from 12 UTC 4 June 2008 to 12 UTC 5 June 2008.

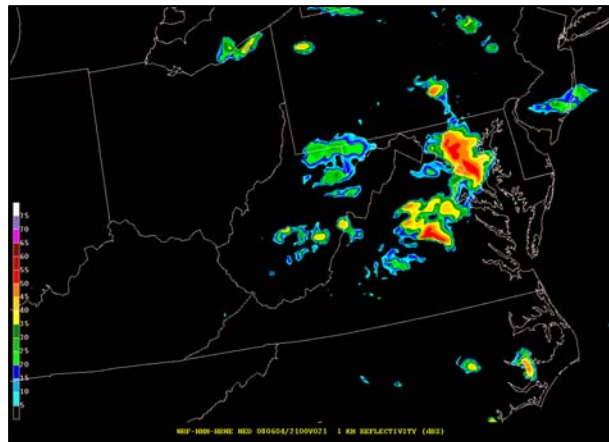


**Figure 14.** 00 UTC 4 June 2008 WRF-NMM 21-hour forecast of simulated reflectivity at 1 km AGL valid 21 UTC 4 June.

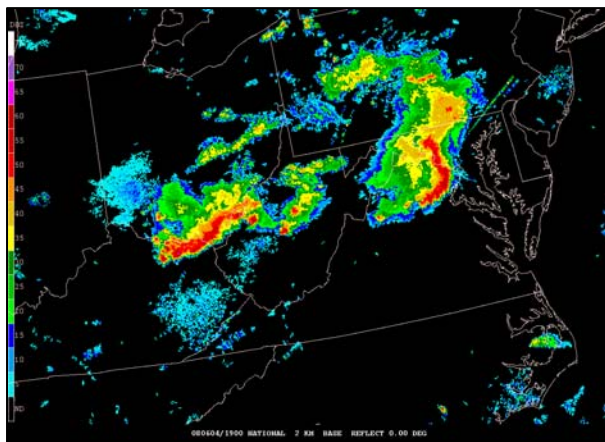


**Figure 12.** Regional radar reflectivity mosaic image at 19 UTC 4 June 2008. Note initial box echo system moving through the Washington, D.C., area.

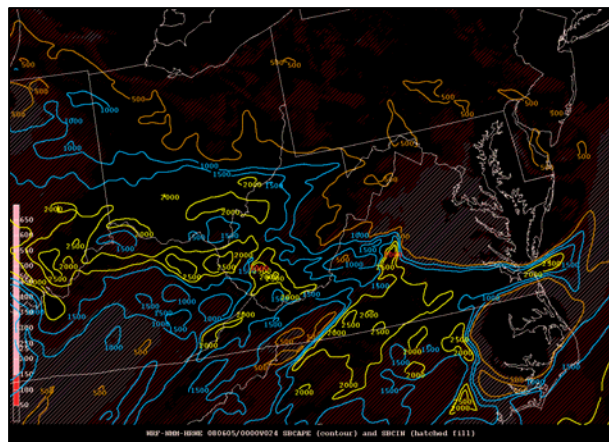


**Figure 15.** 00 UTC 4 June 2008 WRF-NMM 24-hour forecast of surface-based CAPE (contours at  $500 \text{ J kg}^{-1}$  interval) and CIN (hatched color fill) valid 00 UTC 5 June.

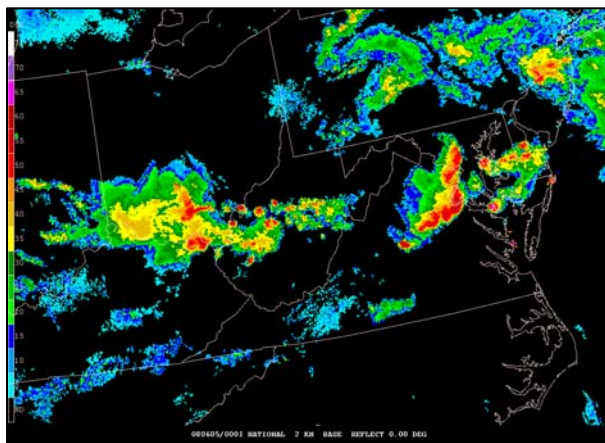


**Figure 13.** Regional radar reflectivity mosaic image at 00 UTC 5 June 2008. Note the second bow echo system moving through the Washington, D.C., area.

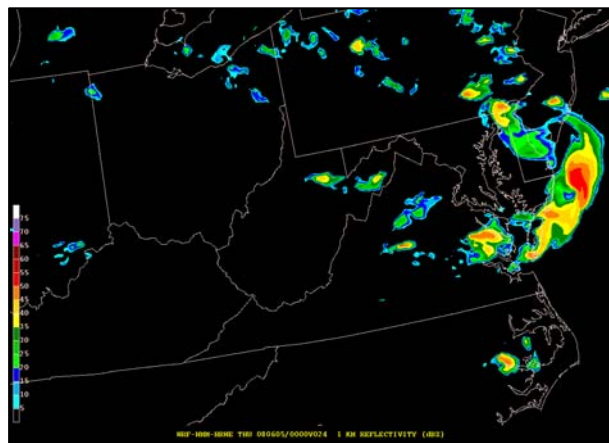


**Figure 16.** 00 UTC 4 June 2008 WRF-NMM 24-hour forecast of simulated reflectivity at 1 km AGL valid 00 UTC 5 June.



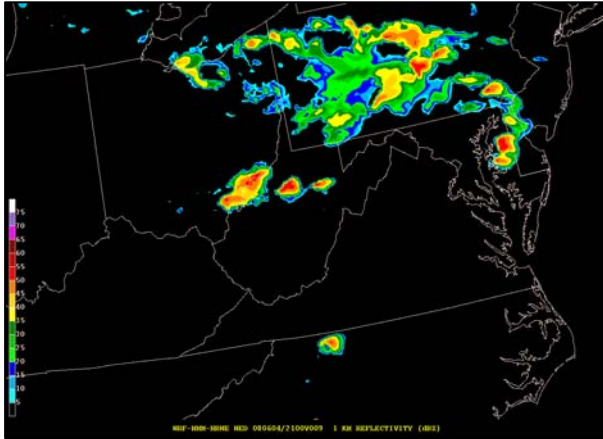


**Figure 17.** 12 UTC 4 June 2008 WRF-NMM 9-hour forecast of simulated reflectivity at 1 km AGL valid 21 UTC 4 June..

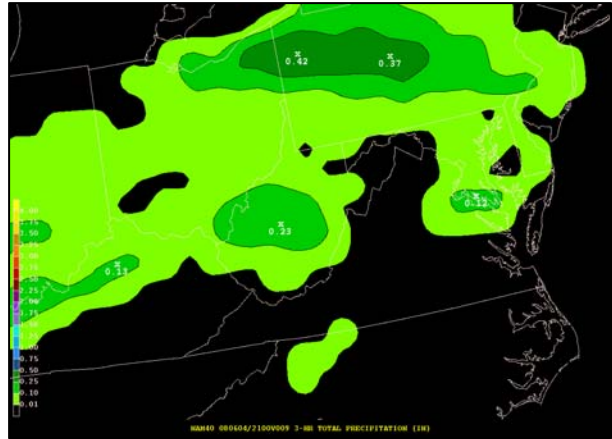


**Figure 20.** 12 UTC NAM 9-hour forecast of 3-hour accumulated precipitation valid 21 UTC 4 June.

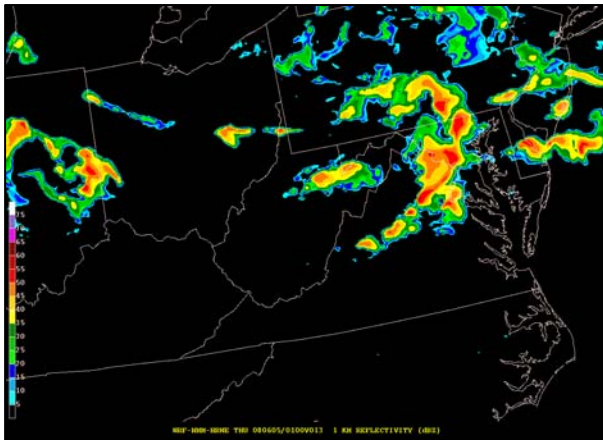


**Figure 18.** 12 UTC 4 June 2008 WRF-NMM 13-hour forecast of simulated reflectivity at 1 km valid 01 UTC 5 June.

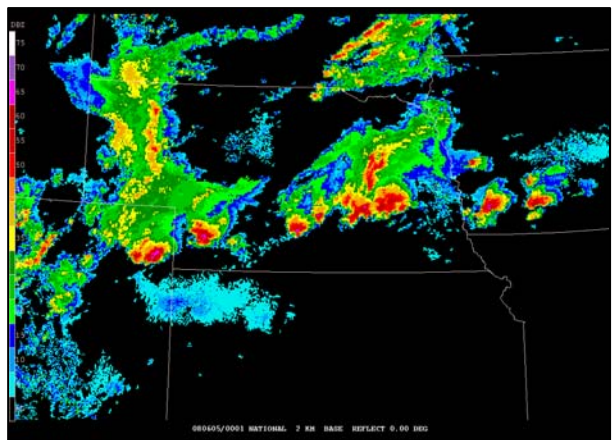


**Figure 21.** Regional radar reflectivity mosaic image at 00 UTC 5 June 2008.

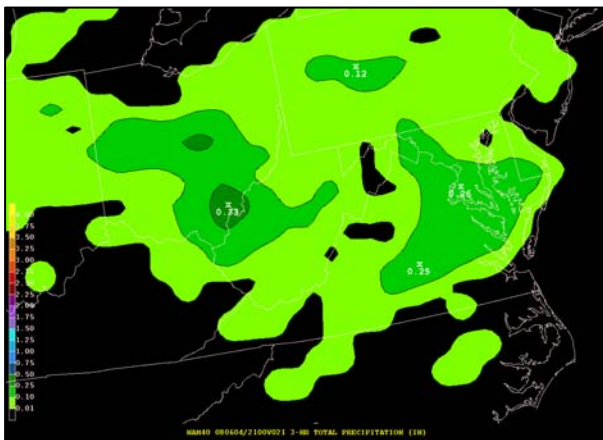


**Figure 19.** 00 UTC NAM 21-hour forecast of 3-hour accumulated precipitation valid 21 UTC 4 June.

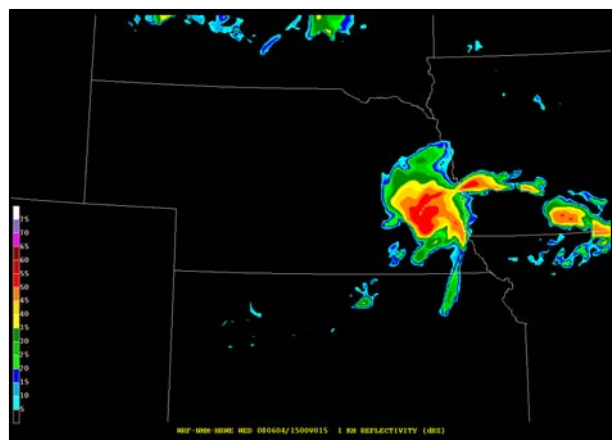


**Figure 22.** 00 UTC 4 June 2008 WRF-NMM 15-hour forecast of simulated reflectivity at 1 km AGL valid 15 UTC 4 June.

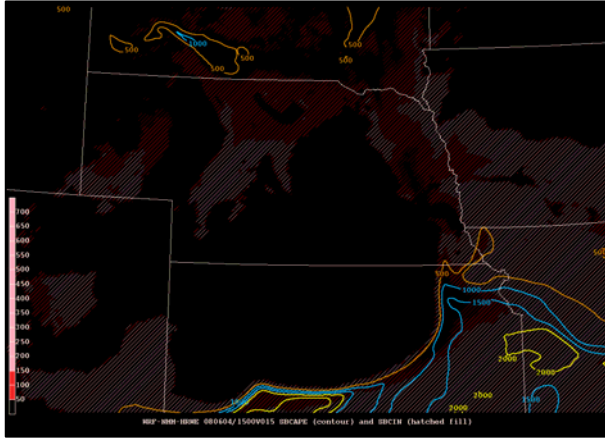


**Figure 23.** 00 UTC 4 June 2008 WRF-NMM 15-hour forecast of surface-based CAPE (contours at 500 J kg<sup>-1</sup> interval) and CIN (hatched color fill) valid 15 UTC 4 June.

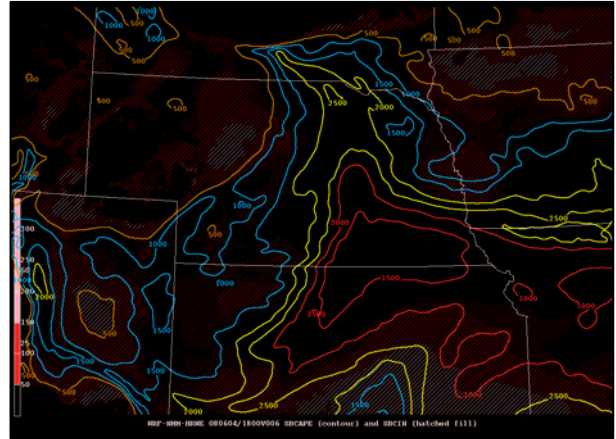


**Figure 26.** 12 UTC 4 June 2008 WRF-NMM 6-hour forecast of surface-based CAPE (contours at 500 J kg<sup>-1</sup> interval) and CIN (hatched color fill) valid 18 UTC 4 June.

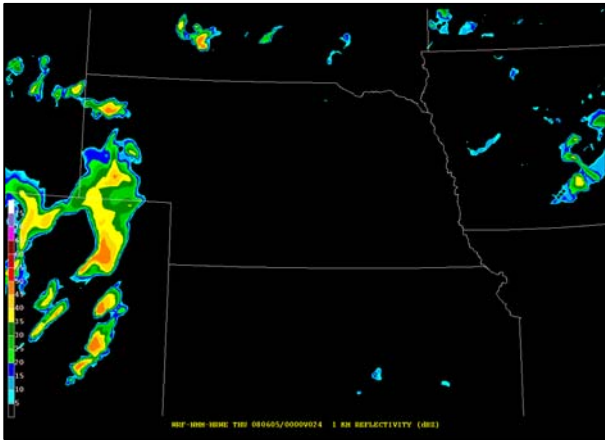


**Figure 24.** 00 UTC 4 June 2008 WRF-NMM 24-hour forecast of simulated reflectivity at 1 km AGL valid 00 UTC 5 June.

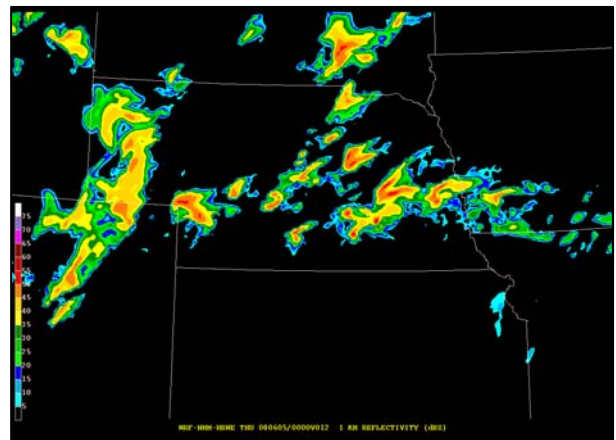


**Figure 27.** 12 UTC 4 June 2008 WRF-NMM 12-hour forecast of simulated reflectivity at 1 km AGL valid 00 UTC 5 June.

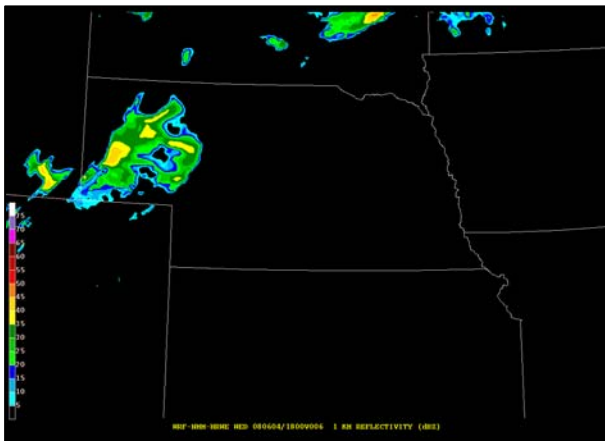


**Figure 25.** 12 UTC 4 June 2008 WRF-NMM 6-hour forecast of simulated reflectivity at 1 km AGL valid 18 UTC 4 June.

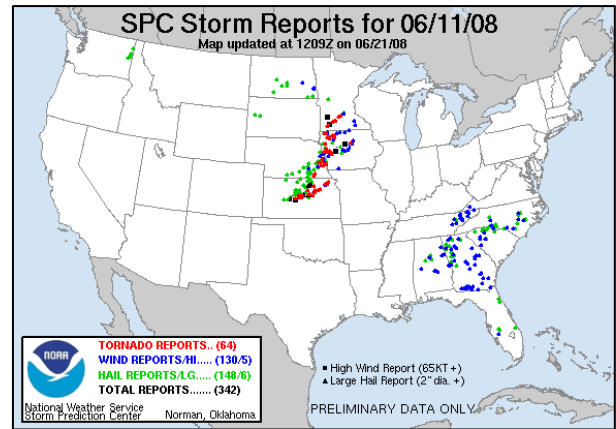


**Figure 28.** Severe weather reports of tornadoes (red), large hail (green), and convective wind damage (blue) from 12 UTC 11 June to 12 UTC 12 June.

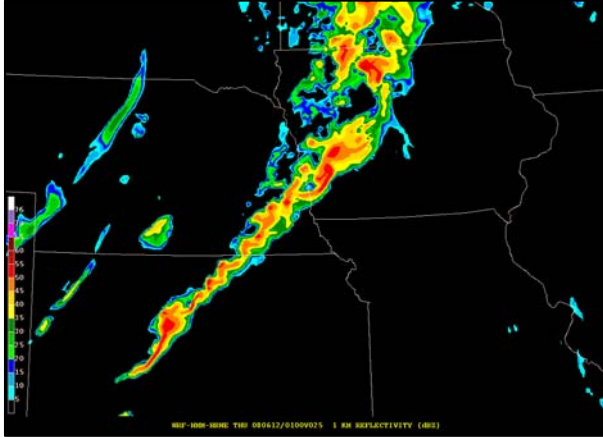


**Figure 29.** 00 UTC 11 June 2008 WRF-NMM 25-hour forecast of simulated reflectivity at 1 km AGL valid 01 UTC 12 June. This is near the time of the killer tornado in western Iowa and 1-2 hours before killer tornadoes in northeast Kansas.



**Figure 32.** 00 UTC 11 June 2008 NAM 27-hour forecast of 3-hour accumulated precipitation valid 03 UTC 12 June.

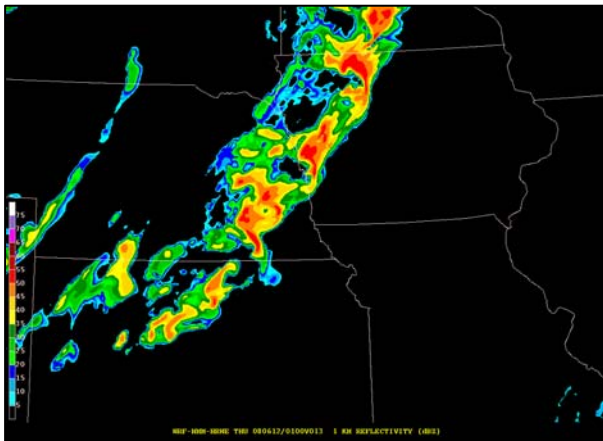


**Figure 30.** 12 UTC 11 June 2008 WRF-NMM 13-hour forecast of simulated reflectivity at 1 km AGL valid 01 UTC 12 June. This is near the time of the killer tornado in western Iowa and 1-2 hours before killer tornadoes in northeast Kansas.

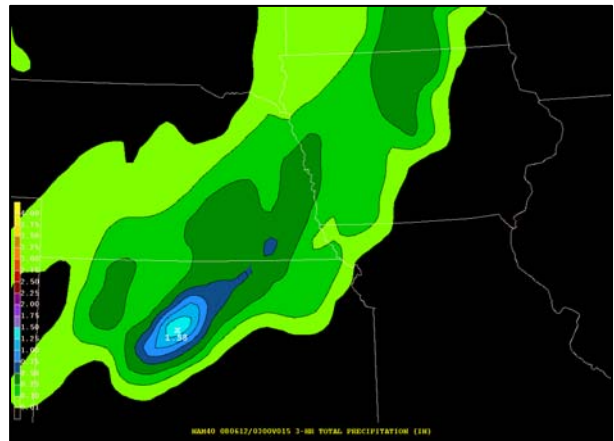


**Figure 33.** 12 UTC 11 June 2008 NAM 15-hour forecast of 3-hour accumulated precipitation valid 03 UTC 12 June.

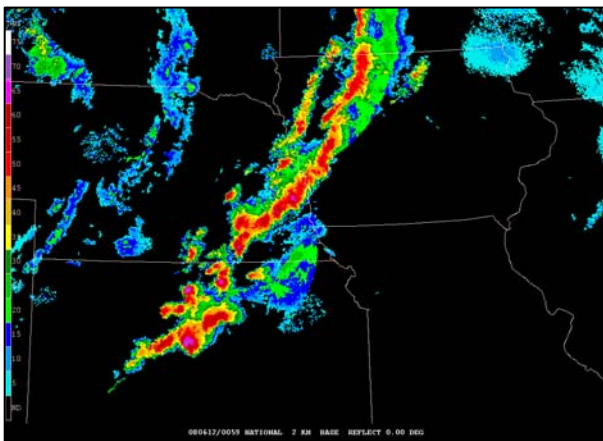


**Figure 31.** Regional radar reflectivity mosaic image at 01 UTC 12 June 2008.